JACS
JOURNAL OF THE AMERICAN CHEMICAL SOCIETY

ARTICLE

pubs.acs.org/JACS

Kinetic Measurements on Single-Molecule Disulfide Bond Cleavage

Jian Liang*,# and Julio M. Fernández*

Department of Biological Sciences, Columbia University, New York, New York 10027, United States

Supporting Information

ABSTRACT: We use single-molecule force clamp spectroscopy (SMFCS) to explore the reactivity of tris(2-carboxyethyl)phosphine (TCEP), 1, 4-DL-dithiothreitol (DTT) and hydrosulfide anion (HS^-) on disulfide bonds within a mechanically stretched polypeptide. The single-bond level bimolecular nucleophilic substitution (S_N2) events are recorded at a series of precisely controlled temperatures so that the Arrhenius kinetic parameters, that is, the height of the activation energy barrier (E_a) and the attempting frequency (A) of the chemical reactions, can be determined. The values of A are typically at the order of 10^7 M^{-1} s^{-1}, which is far lower than that predicted by the transition-state theory, in which A is given by k_BT/h and around 10^{12} M^{-1} s^{-1} at room temperature. Furthermore, E_a is derived to be 30−40 kJ/mol, which can be lowered by ~6−8% with every 100 pN mechanical force applied. The correlation of the A and E_a with the molecular structures reveals that the relative magnitude of these two parameters cannot be simply judged from the size of the molecule or the nucleophilicity of the attacking atom. The comparison of the influences on the reaction rate induced by force and temperature indicates an equivalent accelerating effect by every 50 pN or 10 K increment, giving for the first time the relationship between mechanical and thermal effects on a single-molecule S_N2 chemical reaction.

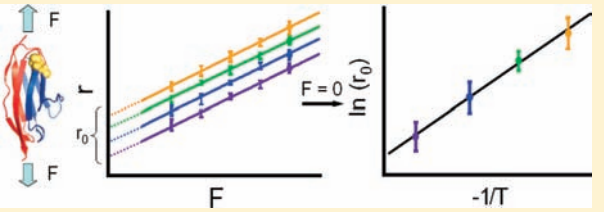

INTRODUCTION

The development of modern experimental techniques allows us to probe chemical reactions from bulk phase down to single-molecule level, which provides numerous new insights into chemistry with unprecedented details. Since late 1980s, single-molecule detection and manipulation, especially those in condensed phase, have become possible with the evolution of various methods such as scanning probe microscopy,[1,2] fluorescence microscopy,[3−5] optical[6,7] and magnetic tweezers,[8,9] and surface-enhanced Raman spectroscopy.[10,11] For instance, Hla et al.[12] demonstrated how to use a scanning tunneling microscope (STM) tip to induce a chemical reaction between two iodobenzene molecules, forming a biphenyl on Cu(111) surface. All the elementary steps of the reaction, including the separation of iodine from the iodobenzene, the collision, and the fusion of the two phenyls, could be controlled by tunneling electrons or mechanical force generated from the tip and could be captured as atomic-resolution images. Compared with bulk-phase chemical reactions, the knowledge on single-molecule chemistry, however, is still far from mature. For instance, a systematic investigation on the kinetic parameters of reactions at single-molecule level, that is, the attempting frequency and the activation energy barrier along the reaction coordinate from which the reaction rate can be fully derived, is largely missing in the literature. Such kinetic measurements have been carried out on several single-molecule processes including protein unfolding,[13] adsorption, and diffusion of fatty acids at the solution/solid interface[14,15] and rotational motion of molecular motors supported on Au surfaces.[16] While these processes may resemble chemical reactions with two states and an activation barrier, they are, however, generally not considered "real" chemical reactions because no breaking or forming of covalent bonds is involved. Recently, we developed a single-molecule force clamp spectroscopy (SMFCS) technique which can probe the rate of S_N2 reactions on disulfide bonds in engineered polyproteins.[17−19] The other mode of atomic force microscope (AFM) based single-molecule force spectroscopy, often referred to as "force extension", has been applied to investigating the mechanical properties of proteins[20−22] and ligand−receptor interactions[23,24] but not able to measure the reaction rate under constant force. In our assay, a polyprotein molecule containing tandem repeats of identical domains is stretched between an AFM tip and the surface of a gold-coated coverslip at a constant force which is precisely controlled in terms of both direction and magnitude. Each domain has a disulfide bond buried in the hydrophobic core of the protein which is not exposed to the solvent in its folded state. In the experiment, as illustrated in Figure 1A−C, the molecule is first stretched to unfold the protein modules and expose the disulfide bonds to the nucleophiles in the solution. Then, for a time period depending on the reaction rate, a second force pulse is applied during which the disulfide bond in each domain is cleaved by the nucleophilic attack. The reduction events release the amino acids within the polypeptide chain trapped by the disulfide bonds and result in stepwise increase of the extension of the molecule along the pulling direction (Figure 1D). These reaction events are recorded as a function of time, and thus, the kinetic measurements on the S_N2 reaction are realized at single-molecule level. Our previous results[17] demonstrated that mechanical force could

Received: October 27, 2010
Published: February 22, 2011

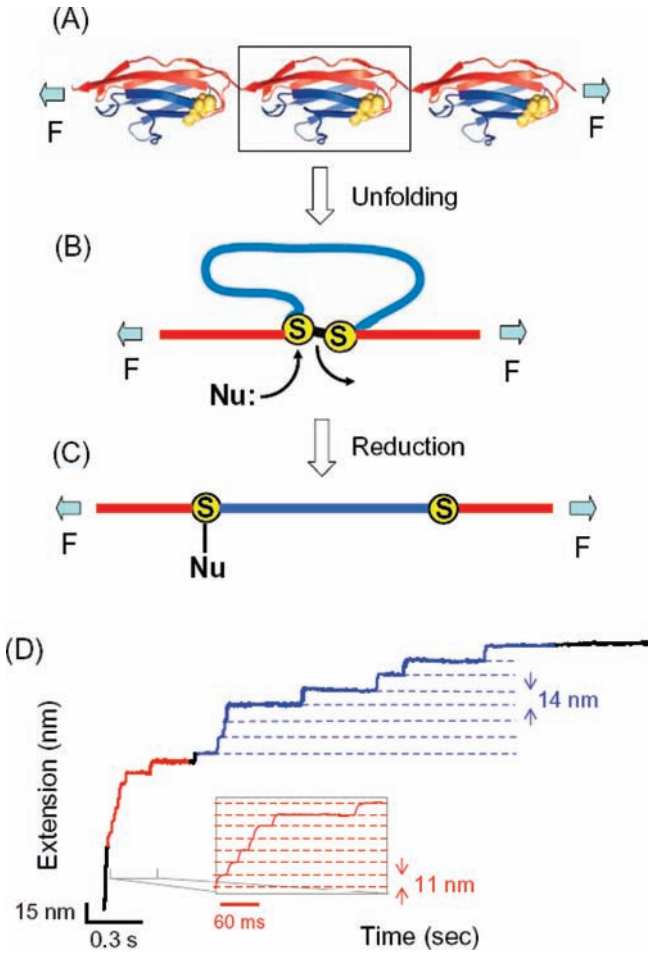

Figure 1. Schematic illustration of the experiment and a typical trace of the SMFCS, marked in different colors (red and blue) as different stages during pulling to guide the eyes. (A) The $(I27_{G32C-A75C})_8$ polyprotein (only three modules are shown) is being stretched between an AFM tip and the substrate. (B) Each $I27_{G32C-A75C}$ domain is unfolded by mechanical force up to the disulfide bond, leaving the amino acids between the 32nd and 75th positions (shown in blue) in a "sequestered" loop and exposing the disulfide bond to the nucleophile. (C) The nucleophile cleaves the disulfide bond which is subjected to constant pulling force, releasing the amino acids in the previously sequestered loop. (D) An actual recording of molecular extension vs time under the double force-pulse protocol, in which the first pulse of 170 pN unfolds the protein modules and the second pulse of 200 pN is applied during the entire reduction process (by TCEP in this case). The red part of the trace contains a quick increment of extension of a series of ~11 nm steps (inset), indicating the unfolding of the domains of the polyprotein. The blue part involves the second set of steps, with ~14 nm height, fingerprinting the disulfide bond reduction events.

catalyze chemical reactions and the reaction rate r could be well described by Bell model[25] in an Arrhenius term of the form:

$$r = A[nucleophile]\exp\left(\frac{F\Delta x_r - E_a}{k_B T}\right) \quad (1)$$

where A is the pre-exponential factor, F is the applied stretching force, E_a is the activation energy barrier, k_B is the Boltzmann constant, and T is the temperature. From Arrhenius fits to the force dependency of the reduction rate, we measured Δx_r, which could be described as the distance to the transition state along the reaction coordinate and was extensively discussed in our previous report.[26] However, from solely the force-dependent data, we were not able to derive A and E_a of these reactions. As a result, we had to arbitrarily calculate E_a which was relying on our choice of value for A (10^{12} M^{-1} s^{-1} estimated from the transition state theory),[26] because in those experiments the two variables could not be measured independently.

In this paper, we use SMFCS to investigate the S_N2 reactions induced by TCEP, DTT, and HS^- on disulfide bonds. Although S_N2 reactions have been identified and investigated in a wide range of organic and biological reactions, the factors influencing their kinetic and mechanistic details are still incompletely understood and generate continuous interest.[27−29] Here, we measure the rate of the reactions at a series of precisely controlled (within ±0.2 K of every assigned value) temperatures between 278 K (5 °C) and 318 K (45 °C), and at each temperature, the stretching forces range from 100 to 300 pN. With this technique, we derive A and E_a for the first time, to the best of our knowledge, for such chemical reactions at single-molecule level. The comparison between the acceleration of the reaction rate induced by increasing temperature and applying force raises interesting results showing the relative efficiency of thermal and mechanical effects on a chemical reaction.

EXPERIMENTAL SECTION

Protein Engineering, Expression, and Purification. The process of expression and purification of the polyproteins has been described extensively elsewhere.[30] In brief, we construct 8 direct tandem repeats of Ig module 27 of the I band of human cardiac titin (I27) in a polyprotein. Through cysteine mutagenesis, we engineer a disulfide bond in each I27 domain between the 32nd and 75th residues by mutating the 32nd glycine (G) and 75th alanine (A) to two cysteines (C). The disulfide bridge is buried in the folded state of the protein (named $I27_{G32C-A75C}$) and not accessible to solvent or the reducing agent.[31]

SMFCS. Our custom-built AFM and the installation of the temperature controller have been described in details elsewhere,[32,33] and a picture of the setup is shown in the Supporting Information (Figure S1). A gold-coated coverslip is glued to a thermoelectric device (Custom Thermoelectric) by heat-conductive paste. The device can covert the input electrical bias to temperature difference between the two sides of it (Peltier effect).[33] The side opposite to the gold coverslip sample is connected to a heatsink, which is placed on top of the piezoelectric tube and has heat exchange with air or a flux of chilling water. The switch between heating and cooling of the sample can be conveniently achieved by changing the polarity of the input voltage. The temperature in the fluid cell is monitored during the whole experiment by a thin-wire thermocouple (Physitemp Instruments, Inc.). The silicon nitride cantilevers (MLCT, Veeco) we use have a typical spring constant of 10−20 pN nm^{-1}, calibrated using the equipartition theorem. Then, 2.5 mM TCEP, 12.5 mM DTT, or 15 mM $Na_2S \cdot 9H_2O$ (all from Sigma-Aldrich) is dissolved in PBS buffer containing 50 mM sodium phosphate and 150 mM NaCl, and the pH of the solution is adjusted to 7.4, 7.4, or 8.6, respectively. At pH 7.4, the concentration of the deprotonated form of TCEP and DTT is 1.0 and 0.2 mM, respectively.[26] At pH 8.6, which is right between the pK_{a1} and pK_{a2} (7.05 and 19, respectively) of H_2S, the sulfide anions are mostly in the form of HS^-.[34] In an actual experiment, ~5 μL of $(I27_{G32C-A75C})_8$ solution is first deposited onto the gold-coated coverslip. The coverslip is then sealed with the liquid cell into which the buffer containing the nucleophile is injected and mixed with the polyprotein. In force-clamp spectroscopy, single $(I27_{G32C-A75C})_8$ protein molecules are stretched by a double-pulse protocol, in which the first pulse at a constant force of 170 pN for 0.3 s unfolds each protein domain, and then the second pulse at an assigned force value between 100 and 300 pN is applied for a period of time that is long enough to allow the disulfide bond reduction events to happen.

dx.doi.org/10.1021/ja109684q | J. Am. Chem. Soc. 2011, 133, 3528–3534

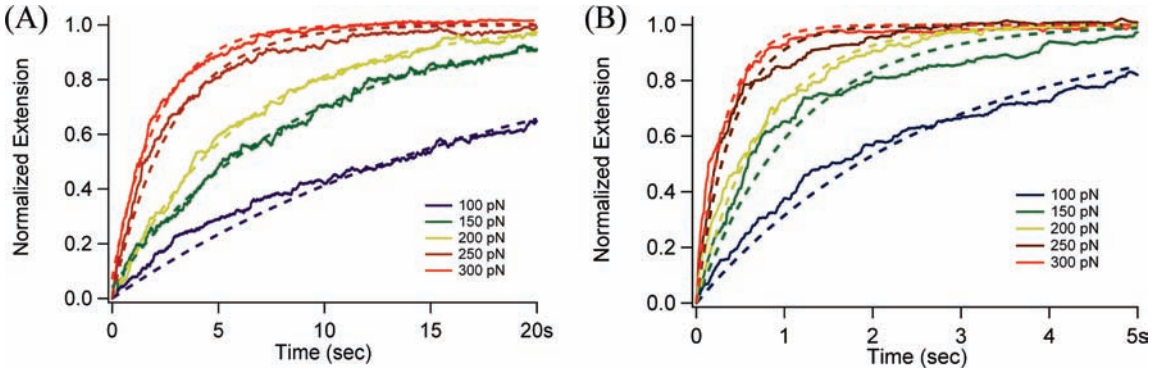

Figure 2. Sets of trace averages ($n > 20$ in each set) of TCEP-induced reduction events as a function of stretching force at (A) 278 K (5 °C) and (B) 318 K (45 °C). The disulfide reduction follows the Markovian behavior (i.e., each reduction event is independent of others) at all temperatures and forces, and consequently the summed up and then normalized traces with reduction steps result in invariant exponential kinetics (eq 2). Single-exponential fits (dotted lines) measure the time constant, τ_r, of the thiol/disulfide exchange, and thus, the reduction rate, $r = 1/\tau_r$, can be derived.

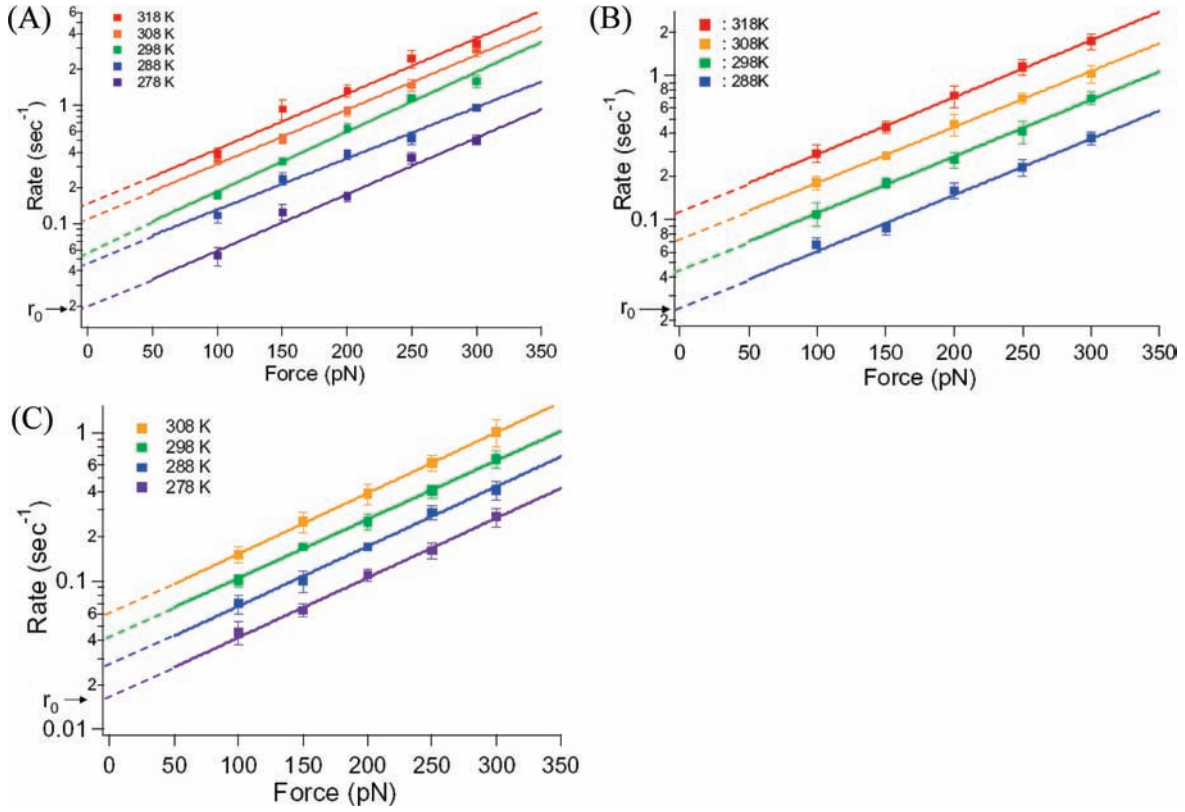

Figure 3. Single-molecule disulfide bond reduction rates as a function of force at different temperatures for (A) TCEP, (B) DTT, and (C) HS^-. The solid lines are the fittings to the data points obtained at the same temperature using the Bell model (eq 1). From the fittings (rate vs force), we acquire $r_0 = A[nucleophile]\exp(-E_a/k_BT)$ at each temperature for different nucleophiles, which will be used for deriving the A and E_a values in Figure 4.

Data Analysis. We collect and analyze data using a custom-written software in IGOR Pro 6 (Wavemetrics). The collected traces (20−30 per data point of measured rate) containing the reduction events are recorded as molecular extension versus time, and the traces obtained at each particular temperature and force are summed and averaged (Figure 2). The resulting averaged traces are fit with single exponential curves using the following equation:

$$P_r(t) = 1 - \exp\left(-\frac{t}{\tau_r}\right) \quad (2)$$

where $P_r(t)$ is the probability of completion of the reduction events, and τ_r is the time constant of the exponential increase from which the reaction rate, $r = 1/\tau_r$, can be derived. The magnitude of the error bars is obtained by bootstrap method. More details about the data analysis procedure can be found in our previous reports.[17,18]

RESULTS AND DISCUSSIONS

1. Deriving A and E_a of the Single-Molecule Reactions. Compared with bulk-phase measurements, SMFCS is probably

dx.doi.org/10.1021/ja109684q | J. Am. Chem. Soc. 2011, 133, 3528–3534

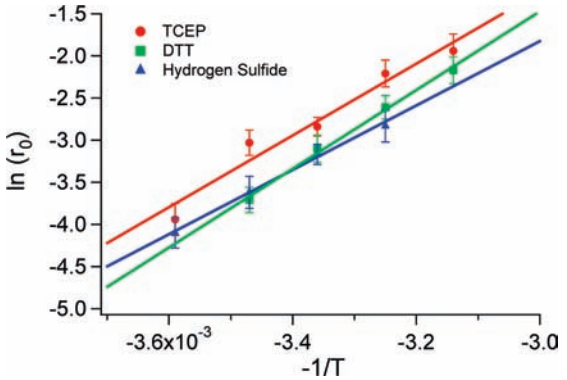

Figure 4. Arrhenius plots of the zero-force rates with temperature. The slope of the fitting (solid lines) gives the activation energy barrier E_a and the extrapolation gives the pre-exponential factor A.

the technique that can derive the reaction rate with the fewest reaction events (typically 10^2, or 10^{-20} mol for each measured rate). Figure 3 demonstrates the rates of the single-molecule S_N2 reactions as functions of both the applied force and temperature. In the semilogarithmic plots, the fitting of the rate with force all agrees quite well with the Bell model (eq 1), and the slope of the fitting lines measures Δx_r (Table S1 in the Supporting Information) which represents the force sensitivity of the reaction. Clearly, in eq 1 the relationship between the reaction rate and temperature regresses to the classical Arrhenius equation when no force is applied:

$$r = r_0 \exp\left(\frac{F\Delta x_r}{k_B T}\right) \quad (3)$$

where

$$r_0 = A[nucleophile]\exp\left(\frac{-E_a}{k_B T}\right) \quad (4)$$

and $r = r_0$ when $F = 0$. It is worth noting that r_0 cannot be directly measured in the experiment because the disulfide bond is buried in the hydrophobic core and not exposed to the nucleophiles when no force is applied and the protein is in its folded state. However, r_0 can be acquired from the fitting of r to F at each temperature, in which r_0 can be interpreted as the extrapolation of the rate data to the zero-force point. After collecting all the values of r_0 at different temperatures, we plot $\ln[r_0(T)]$ as a function of $-1/T$ using eq 4, as illustrated in Figure 4. These classical Arrhenius fits give the A and E_a values for each S_N2 reaction that is listed in Table 1.

Strikingly, the measured values of A are all quite low (10^5–10^{10}), especially compared with that calculated from the transition-state theory[35] in which A is given by k_BT/h, where h is the Planck constant. This frequency represents the number of trials of converting the reactants to the product and should be around 10^{12} s^{-1} at room temperature. This result suggests that the transmission coefficient, that is, the probability of each trial leading to the formation of the product, is rather small in the reactions. First, we can exclude the possibility that the measured rate is diffusion-limited because the diffusion of the nucleophiles does not rely on the applied force on the substrate and consequently cannot account for the force-dependent nature of the reaction. Such low attempting frequencies imply that there are some conditions other than simple collisions that need to be fulfilled to allow the chemical reaction to proceed. Iglesia et al.[36]

Table 1. Kinetic Parameters Measured on the S_N2 Reactions

Nucleophile	Molecular structure	A ($M^{-1}sec^{-1}$)	E_a (kJ/mol)
TCEP	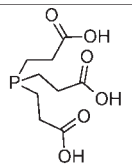	$10^{8.01\pm0.76}$ ($1.8 \times 10^7 - 5.9 \times 10^8$)	35 ± 4
DTT	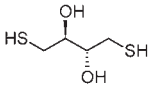	$10^{9.14\pm0.90}$ ($1.8 \times 10^8 - 1.1 \times 10^{10}$)	39 ± 5
Hydrosulfide anion	HS^-	$10^{6.01\pm1.05}$ ($9.1 \times 10^4 - 1.1 \times 10^7$)	32 ± 6

pointed out that a unimolecular reaction typically had a high A value which was close to that predicted by the transition-state theory. In contrast, bimolecular reactions often involve subtle rearrangements of the reactant molecules to form the activated complex, adding more restrictive conditions for a successful conversion. For instance, S_N2 reactions require back-side attack to satisfy the ~180° angle at the transition state between the nucleophilic atom, the electron-deficient center, and the leaving group. Furthermore, in aqueous solutions, the synchronous desolvation of the reactant molecules is a prerequisite for the nucleophilic attack to happen. Such multistep selections may dramatically reduce the measured attempting frequency. Another evidence supporting this proposal is that the A values measured in gas phase[37] are often close to those predicted by the transition-state theory. Interestingly, the A values of reactions of molecules adsorbed on solid surfaces are usually high when the coverage is low, but would be reduced by orders of magnitude when the coverage is high and the interactions between molecules are not negligible. The former case resembles the unimolecular reaction while the latter one confirms that the requirement of concerted action of multiple molecules can lower the probability of the reactants going onto the correct reaction trajectory. For instance, the A values of H_2 desorption from Ni surface were measured to be 10^{13}–10^{15} s^{-1} and 10^6–10^{11} s^{-1} at low and high coverages, respectively.[37] Another example is that the A value of unimolecular formic acid decomposition on copper surface is ~10^{13}–10^{14} s^{-1}, while the pseudo-first-order A for the same reaction but through a bimolecular mechanism is only ~10^{10} s^{-1} when the coverage exceeds 20%.[36] Baber et al.[16] measured the attempting frequency of rotation of single-molecule thioethers on gold surfaces to be at the order of 10^7. The authors hypothesized that the synchronous motion of both rotor arms was necessary for the molecular rotation, suggesting such constraint to the reaction could lower the A value.

2. Steric Effect and Electronic Effect on the A and E_a Values. The steric effect usually refers to the existence of bulky groups in the vicinity of the nucleophilic atom or the electron-deficient center which can reduce the chance of collision between them. However, in Table 1, the measured A value of the reaction induced by TCEP (10^7–10^8) is slightly higher than that induced by HS^- (10^5–10^7), although in the former molecule the phosphorus atom is chemically bonded with three carboxyethyl groups while the latter is a much smaller nucleophile, suggesting

dx.doi.org/10.1021/ja109684q | J. Am. Chem. Soc. 2011, 133, 3528–3534

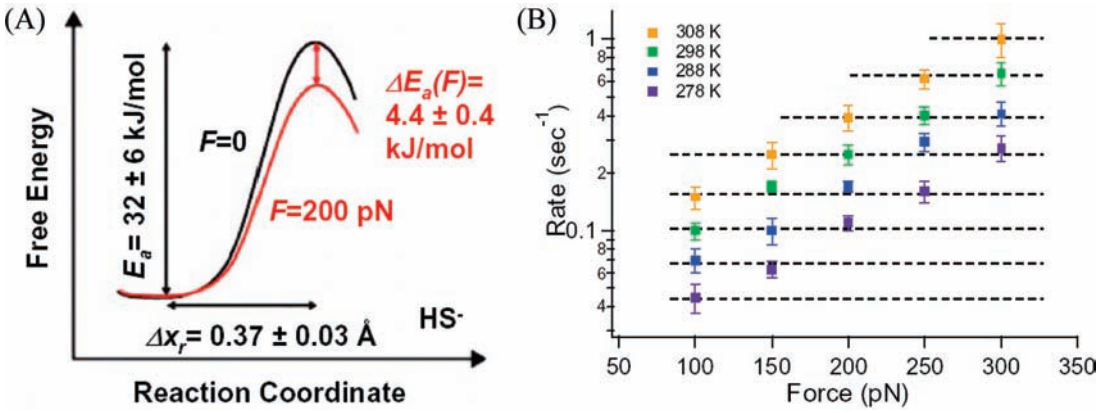

Figure 5. (A) Simplified illustration of the free energy landscape of HS^- initiated disulfide-bond reduction. The measured E_a for the reaction at zero force is 32 ± 6 kJ/mol, which can be lowered by 4.4 ± 0.4 kJ/mol (14%) at an applied force of 200 pN. (B) The same data set as shown in Figure 3C but with iso-rate lines indicating that 50 pN and 10 K have similar effect on the acceleration of the reaction.

that the spatial hindrance is not of substantial importance in these reactions. Another interesting comparison between DTT and HS^- reveals that, although DTT is a bulkier molecule, the A value of DTT (10^8–10^{10}) is 3 orders of magnitude higher than that of HS^-. When DTT approaches the disulfide bond, either of its two −SH groups can perform the nucleophilic attack, leading to a much higher attempting frequency.

Besides A, the E_a value is also correlated with the molecular structure. Usually, this effect is evaluated by the nucleophilicity of the atom that attacks the target bond. The data in Table 1 demonstrate that the E_a values of the reactions are between 30 and 40 kJ/mol, close to those calculated using density functional theory (~11 kcal/mol).[38] These E_a values are significantly lower than the barrier of S_N2 reactions between halide anions and alkyl halides obtained from either theoretical calculation or experimentation,[39,40] which is consistent with the fact that sulfur and phosphorus are much better nucleophiles than halogens. Interestingly, although the phosphorus atom has smaller electronegativity than sulfur, the E_a values of the TCEP and HS^- induced S_N2 reactions are very similar to each other while that of DTT is slightly higher. More likely, the activation energy is determined by multiple factors when the difference in intrinsic nucleophilicity is small. For instance, the electron-pulling groups in TCEP and DTT (−COOH and −OH, respectively) may reduce the nucleophilicity of the molecules, and consequently, the E_a of TCEP increases to the same level as HS^- and that of DTT is higher than HS^-.

3. Comparison between the Thermal Effect and the Mechanical Effect on the S_N2 Reactions. As illustrated in eq 1 and Figure 5A, the applied force can lower the activation barrier by an amount of $F\Delta x_r$. Table S1 lists all the Δx_r values for the S_N2 reactions at different temperatures. Notably, the Δx_r value increases slightly with temperature, implying the position of the transition state moves further away from the reactant (or closer to the product) along the reaction coordinate.[41] One possible explanation is that the S_N2 reactions in our experiments are entropy-reduced processes because the nucleophile is covalently bonded to one of the sulfur atoms in the initial disulfide bridge, leading to reduction of the total number of molecules (Figure 1B,C). As a result, increasing temperature will raise the free energy of the product with respect to the reactants and lead to the shift the transition state toward the product and the gain of Δx_r. In summary, with the response of the reaction rate to the applied force, it is possible to probe the *position* of the transition state along the reaction coordinate.

Given the values of E_a, we can compare the thermal effect and mechanical effect on the S_N2 reactions using eq 1:

$$\ln\frac{r_2}{r_1} = \frac{E_a}{k_B}\left(\frac{T_2 - T_1}{T_2 T_1}\right) = \frac{\Delta x_r}{k_B T}(F_2 - F_1) \qquad (5)$$

where the rate change (r_2/r_1) is equally induced by temperature or force. If the temperature variation is small, we have $T_1T_2 \approx T^2$ and then eq 5 can be further simplified as:

$$\frac{(F_2 - F_1)\Delta x_r}{E_a} = \frac{T_2 - T_1}{T} \qquad (6)$$

Equation 6 shows that, when the thermally and the mechanically induced accelerating effects are similar, the ratio of the apparent mechanical work to the activation energy should be equal to the relative temperature change. As an example, Figure 5B demonstrates straightforwardly that for the HS^- induced thiol−disulfide exchange, the effects resulting from 10 K increment in temperature or 50 pN in force are similar to each other [e.g., r(288 K, 100 pN) ≈ r(278 K, 150 pN), r(298 K, 100 pN) ≈ r(288 K, 150 pN) ≈ r(278 K, 200 pN), and so on]. This phenomenon can be rationalized by the fact that the Δx_r value is measured to be around 0.3–0.5 Å, and as a result, $F\Delta x_r$ is calculated to be ~1.2 kJ/mol at the force of 50 pN, which is around 3% of the activation energy barrier. This number is in accordance with the relative temperature change in which 10 K is roughly 3% of room temperature (298 K). Using eq 1, one can also calculate how much the energy barrier is lowered at any given force. For instance, at 500 pN, E_a is lowered by ~30% which is not trivial. In our previous reports,[42] we observed that, at ~500 pN, the force dependency of the reaction rate showed a turning point above which the force acceleration effect was greatly diminished. Although the direct lengthening of the disulfide bond by the stretching force is rather small,[42] other conformational changes, such as the dihedral angle distortion, may significantly affect the reactivity of the disulfide bond.

■ CONCLUSIONS AND OUTLOOK

We have shown that temperature-variation SMFCS is a powerful tool for kinetic measurements on reactions of individual chemical bonds. The results demonstrate that the Arrhenius

pre-exponential factor (A) and the activation energy barrier (E_a) can be derived unambiguously: (1) The A values of the S_N2 reactions are much lower than the vibrational frequency along the reaction coordinate, indicating more strict selection rules, including the necessity to remove the solvation shell from the reactant molecules and to search the correct geometries to perform the nucleophilic attack, are important factors in the formation of the activated complex; (2) The relative magnitude of the attempting frequency cannot be simply judged from the size of the nucleophiles. More importantly, if there are more than one functional groups that can perform the nucleophilic attack, the apparent attempting frequency would likely be shifted to higher values; (3) E_a is not solely determined by the electronegativity of the nucleophilic atom, but rather, together by the solvation effect and the structure of the whole molecule. Attention should be paid to electron drawing/donating groups even when they are not directly bonded to the central atom.

The comparison between the acceleration of the reaction caused by increasing temperature and by applying force indicates that every 50 pN and 10 K result in roughly equivalent effect on the rate increment of the HS^- induced thiol−disulfide exchange. Future work in our lab should include constructing other mutants of I27 with the disulfide bond at different positions (other than 32−75) and testing their reactivities to figure out the effect of the proximate amino acids. Interestingly, although our report has been focusing on S_N2 reactions on disulfide bonds, the technique can be applied to, in principle, any other chemical reactions with bond rupture. Because of the variety of mechanisms for different reactions, we expect that the force dependency of the rates would be rather diversified since the configurations of the molecules at the transition state would determine how much the mechanical work could lower the activation energy barrier. Such measurement should preferably be performed at single-molecule level because of the difficulty in aligning the randomly oriented molecules in bulk phase along the force coordinate. Consequently, with proper design of the molecule with desired reactivity, this technique can greatly help understand the force effects on various chemical reactions, and can provide new insights into the fundamental mechanisms of these reactions as well.

■ ASSOCIATED CONTENT

Supporting Information. A supplementary figure showing our atomic force microscope and a table listing the Δx_r values for all the nucleophiles at different temperatures. This material is available free of charge via the Internet at http://pubs.acs.org.

■ AUTHOR INFORMATION

Corresponding Author

jliang@temple.edu; jfernandez@columbia.edu

Present Addresses

[#]Department of Biology, Temple University.

■ ACKNOWLEDGMENT

We thank Dr. R. I. Hermans and T.-L. Kuo for their help in building the AFM and we acknowledge other members of the Fernández laboratory for critical reading and helpful discussions on the manuscript. This work was supported by NIH Grants HL66030 and HL61228 (to J.M.F.).

■ REFERENCES

(1) Eigler, D. M.; Schweizer, E. K. *Nature* **1990**, *344*, 524.
(2) Rief, M.; Gautel, M.; Oesterhelt, F.; Fernández, J. M.; Gaub, H. E. *Science* **1997**, *276*, 1109.
(3) Xie, X. S.; Trautman, J. K. *Annu. Rev. Phys. Chem.* **1998**, *49*, 441.
(4) Weiss, S. *Science* **1999**, *283*, 1676.
(5) Zhuang, X.; Bartley, L. E.; Babcock, H. P.; Russell, R.; Ha, T.; Herschlag, D.; Chu, S. *Science* **2000**, *288*, 2048.
(6) Bustamante, C.; Smith, S. B.; Liphardt, J.; Smith, D. *Curr. Opin. Struct. Biol.* **2000**, *10*, 279.
(7) Abbondanzieri, E. A.; Greenleaf, W. J.; Shaevitz, J. W.; Landick, R.; Block, S. M. *Nature* **2005**, *438*, 460.
(8) Smith, S. B.; Finzi, L.; Bustamante, C. *Science* **1992**, *258*, 1122.
(9) Strick, T. R.; Croquette, V.; Bensimon, D. *Nature* **2000**, *404*, 901.
(10) Kneipp, K.; Wang, Y.; Kneipp, H.; Perelman, L. T.; Itzkan, I.; Dasari, R.; Feld, M. S. *Phys. Rev. Lett.* **1997**, *78*, 1667.
(11) Nie, S. M.; Emery, S. R. *Science* **1997**, *275*, 1102.
(12) Hla, S.-W.; Bartels, L.; Meyer, G.; Rieder, K.-H. *Phys. Rev. Lett.* **2000**, *85*, 2777.
(13) Schlierf, M.; Rief, M. *J. Mol. Biol.* **2005**, *354*, 497.
(14) Honciuc, A.; Howard, A. L.; Schwartz, D. K. *J. Phys. Chem. C* **2009**, *113*, 2078.
(15) Honciuc, A.; Harant, A. W.; Schwartz, D. K. *Langmuir* **2008**, *24*, 6562.
(16) Baber, A. E.; Tierney, H. L.; Sykes, E. C. H. *ACS Nano* **2008**, *2*, 2385.
(17) Wiita, A. P.; Ainavarapu, S. R. K.; Huang, H. H.; Fernández, J. M. *Proc. Natl. Acad. Sci. U.S.A.* **2006**, *103*, 7222.
(18) Wiita, A. P.; Perez-Jimenez, R.; Walther, K. A.; Gräter, F.; Berne, B. J.; Holmgren, A.; Sanchez-Ruiz, J. M.; Fernández, J. M. *Nature* **2007**, *450*, 124.
(19) Liang, J.; Fernández, J. M. *ACS Nano* **2009**, *3*, 1628.
(20) Bustanji, Y.; Samorì, B. *Angew. Chem., Int. Ed.* **2002**, *41*, 1546.
(21) Brown, A. E. X.; Litvinov, R. I.; Discher, D. E.; Weisel, J. W. *Biophys. J.* **2007**, *92*, L39.
(22) Peng, Q.; Li, H. B. *J. Am. Chem. Soc.* **2010**, *131*, 13347.
(23) Kersey, F. R.; Yount, W. C.; Craig, S. L. *J. Am. Chem. Soc.* **2006**, *128*, 3886.
(24) Guo, S. L.; Li, N.; Lad, N.; Ray, C.; Akhremitchev, B. B. *J. Am. Chem. Soc.* **2010**, *132*, 9681.
(25) Bell, G. I. *Science* **1978**, *200*, 618.
(26) Ainavarapu, S. R. K.; Wiita, A. P.; Dougan, L.; Uggerud, E.; Fernández, J. M. *J. Am. Chem. Soc.* **2008**, *130*, 6479.
(27) Sun, L. P.; Song, K. Y.; Hase, W. L. *Science* **2002**, *296*, 875.
(28) Mikosch, J.; Trippel, S.; Eichhorn, C.; Otto, R.; Lourderaj, U.; Zhang, J. X.; Hase, W. L.; Weidemuller, M.; Wester, R. *Science* **2008**, *319*, 183.
(29) Fernández, I.; Frenking, G.; Uggerud, E. *Chem.—Eur. J.* **2009**, *15*, 2166.
(30) Carrion-Vazquez, M.; Oberhauser, A. F.; Fisher, T. E.; Marszalek, P. E.; Li, H. B.; Fernández, J. M. *Prog. Biophys. Mol. Biol.* **2000**, *74*, 63.
(31) Ainavarapu, S. R. K.; Wiita, A. P.; Huang, H. H.; Fernández, J. M. *J. Am. Chem. Soc.* **2008**, *130*, 436.
(32) Schlierf, M.; Li, H.; Fernández, J. M. *Proc. Natl. Acad. Sci. U.S.A.* **2004**, *101*, 7299.
(33) Yang, Y.; Lin, F. C.; Yang, G. L. *Rev. Sci. Instrum.* **2006**, *77*, 5.
(34) Lide, D. R., Ed.; *CRC Handbook of Chemistry and Physics*, 90th ed. (Internet Version 2010); CRC Press/Taylor and Francis: Boca Raton, FL, 2009; pp 8−40.
(35) Laidler, K. J.; Glasston, S.; Eyring, H. *J. Chem. Phys.* **1940**, *8*, 659.
(36) Iglesia, E.; Boudart, M. *J. Phys. Chem.* **1986**, *90*, 5272.
(37) Zhdanov, V. P. *Surf. Sci. Rep.* **1991**, *12*, 183.

(38) Dmitrenko, O.; Thorpe, C.; Bach, R. D. *J. Org. Chem.* **2007**, *72*, 8298.
(39) Chandrasekhar, J.; Smith, S. F.; Jorgensen, W. L. *J. Am. Chem. Soc.* **1984**, *106*, 3049.
(40) Shaik, S. S. *J. Am. Chem. Soc.* **1984**, *106*, 1227.
(41) Tinoco, I., Jr.; Bustamante, C. *Biophys. Chem.* **2002**, *101*−*102*, 513.
(42) Garcia-Manyes, S.; Liang, J.; Szoszkiewicz, R.; Kuo, T.-L.; Fernández, J. M. *Nat. Chem.* **2009**, *1*, 236.